

SCIENTIFIC REPORTS



OPEN

Huygens synchronization of two clocks

Henrique M. Oliveira^{1,*} & Luís V. Melo^{2,*}

Received: 30 January 2015

Accepted: 12 May 2015

Published: 23 July 2015

The synchronization of two pendulum clocks hanging from a wall was first observed by Huygens during the XVII century. This type of synchronization is observed in other areas, and is fundamentally different from the problem of two clocks hanging from a moveable base. We present a model explaining the phase opposition synchronization of two pendulum clocks in those conditions. The predicted behaviour is observed experimentally, validating the model.

The synchronization between two periodic systems connected through some form of coupling is a recurrent, and still pertinent, problem in Nature, and in particular in Physics. During the 17th century Huygens, the inventor of the pendulum clock, observed phase or phase opposition coupling between two heavy pendulum clocks hanging either from a house beam and later from a board sitting on two chairs¹. These two systems are inherently different in terms of the coupling process, and in consequence of the underlying model. The later case has been thoroughly studied^{2–9} by considering momentum conservation in the clocks-beam system. The first case has been approached in theoretical works^{10–13}. We present a mathematical model where the coupling is assumed to be attained through the exchange of impacts between the oscillators (clocks). This model presents the additional advantage of being independent of the physical nature of the oscillators, and thus can be used in other oscillator systems where synchronization and phase locking has been observed¹⁴. The model presented starts from the Andronov¹⁵ model of the phase-space limit cycle of isolated pendulum clocks and assumes the exchange of single *impacts* (sound solitons, for this system) between the two clocks at a specific point of the limit cycle. Two coupling states are obtained, near phase and near phase opposition, the latter being stable. Our experimental data, obtained using a pair of similar pendulum clocks hanging from an aluminum rail fixed to a masonry wall, match the theoretical predictions and simulations.

Andronov model

The model for the isolated pendulum clock has been studied using models with viscous friction by physicists^{2,3,5–9}. However, Russian mathematicians lead by Andronov published a work¹⁵ where the stability of the model with dry friction is established (*Andronov clock*). The authors prove the existence and stability of the limit cycle.

We adopt as basis for our work the first of the aforementioned models, assuming that dry friction predominates. Using the angular coordinate q , the differential equation governing the pendulum clock is

$$\ddot{q} + \mu \operatorname{sign} \dot{q} + \omega^2 q = 0, \quad (1)$$

where $\mu > 0$ is the dry friction coefficient, ω is the natural angular frequency of the pendulum and $\operatorname{sign}(x)$ a function giving -1 for $x < 0$ and 1 for $x > 0$ and $\operatorname{sign} 0 \in [-1, 1]$. In¹⁵ was considered that, in each cycle, a fixed amount of normalized kinetic energy $\frac{h^2}{2}$ is given by the escape mechanism to the pendulum to compensate the loss of kinetic energy due to dry friction in each complete cycle. We call to the transfer

¹Center of Mathematical Analysis Geometry and Dynamical Systems, Department of Mathematics, Técnico, Universidade de Lisboa, Av. Rovisco Pais, 1049-001, Lisboa, Portugal. ²INESC-MN and IN, Av. Alves Redol 9, 1000-029 Lisboa, Portugal and Department of Physics, Técnico, Universidade de Lisboa, Av. Rovisco Pais, 1049-001, Lisboa, Portugal. *These authors contributed equally to this work. Correspondence and requests for materials should be addressed to H.M.O. (email: holiv@math.tecnico.ulisboa.pt)

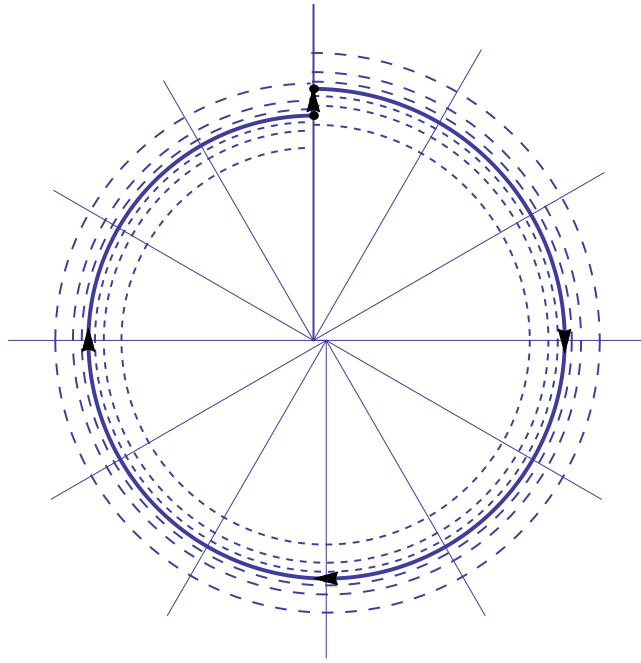


Figure 1. Limit cycle of an isolated clock represented as a solid curve in the phase space. Horizontal axis represents the angular position and in the vertical axis the velocity. We use normalized coordinates to get arcs of circles.

of kinetic energy a *kick*. We set the origin such that the kick is given when $q = -\frac{\mu}{\omega^2}$, which is very close to 0. The phase portrait is shown in Fig. 1.

There are anchors with geometries allowing two symmetric kicks per cycle. The theoretical treatment is similar but we adopted the first model, with one kick per cycle, due to the geometry of the anchor of the clocks used in the experimental setting.

Considering initial conditions $q(t=0) = -\frac{\mu}{\omega^2}$ and $\dot{q}(t=0) = v_0$, we draw a Poincaré section (¹⁶ vol. II, page 268) as the half line $q = -\frac{\mu}{\omega^2}^+$ and $\dot{q} > 0$ ¹⁵. The symbol + refers to the fact that we are considering that the section is taken immediately after the kick. There is a loss of velocity $-\frac{4\mu}{\omega}$ due to friction during a complete cycle. Considering $v_n = \dot{q}\left(\frac{2n\pi}{\omega}^+\right)$ the velocity at the Poincaré section in each cycle one obtains¹⁵ the non-linear discrete dynamical system

$$v_{n+1} = \sqrt{\left(v_n - \frac{4\mu}{\omega}\right)^2 + h^2}, \quad (2)$$

which has the asymptotically stable fixed point

$$v_f = \frac{h^2\omega}{8\mu} + \frac{2\mu}{\omega}. \quad (3)$$

The fixed point (2) attracts initial conditions v_0 in the interval $\left(\frac{4\mu}{\omega^2}, +\infty\right)$.

Model for two pendulum clocks

We consider two pendulum clocks suspended at the same wall. When one clock receives the kick, the impact propagates in the wall slightly perturbing the second clock. The perturbation is assumed instantaneous since the time of travel of sound in the wall between the clocks is assumed very small compared to the period. The interaction was studied geometrically and qualitatively by Abraham^{10,11}. However, that approach does not give estimates on the speed of convergence.

In Vassalo-Pereira¹³, the theoretical problem of the phase locking is tackled. The author makes the assumptions:

1. Dry friction.
2. The pendulums have the same exact natural frequency ω .
3. The perturbation in the momentum is always in the same vertical direction in the phase space, see also^{10,11}.

4. The perturbation imposes a discontinuity in the momentum but not a discontinuity in the dynamic variable.
5. The interaction between clocks takes the form of a Fourier series¹².

Vassalo-Pereira deduced that the two clocks synchronize with zero phase difference. This is the exact opposite of Huygens first remarks¹ and our experimental observations, where phase opposition was observed. Therefore, we propose here a modified model accounting for a difference in frequency between the two clocks.

Consider two oscillators indexed by $i = 1, 2$. Each oscillator satisfies the differential equation

$$\ddot{q}_i + \mu_i \text{sign} \dot{q}_i + \omega_i^2 q_i = -\alpha_i F(q_j), \text{ for } i, j = 1, 2, i \neq j, \quad (4)$$

when $q_i = -\frac{\mu_i}{\omega_i^2}$, the kinetic energy of each oscillator is increased by the fixed amount h_i as in the *Andronov model*. The coupling term is the normalized force $-\alpha_i F(q_j)$, where F is the interaction function and α_i a constant with acceleration dimensions.

We consider that the effect of the interaction function F is to produce an increment $-\alpha$ in the velocity of each clock leaving the position invariant when the other is struck by the energy kick, as we will see in equations (9). We could consider that the interaction function is the Dirac delta distribution $\delta\left(q_j + \frac{\mu_j}{\omega_j^2}\right)$, giving exactly the same result.

The sectional solutions of the differential equation (4) are obtainable when the clocks do not suffer kicks. To treat the effect of the kicks we construct a discrete dynamical system for the phase difference. The idea is similar to the construction of a Poincaré section. If there exists an attracting fixed point for that dynamical system, the phase locking occurs.

Our assumptions are

1. Dry friction.
2. The pendulums have natural angular frequencies ω_1 and ω_2 near each other with $\omega_1 = \omega + \varepsilon$ and $\omega_2 = \omega - \varepsilon$, where $\varepsilon \geq 0$ is a small parameter.
3. The perturbation in the momentum is always in the same vertical direction in the phase space^{10,11}.
4. Since the clocks have the same construction, the energy dissipated at each cycle of the two clocks is the same, $h_1 = h_2 = h$. The friction coefficient is the same for both clocks, $\mu_1 = \mu_2 = \mu$.
5. The perturbative interaction is instantaneous. This is a reasonable assumption, since in general the perturbation propagation time between the two clocks is several orders of magnitude lower than the periods.
6. The interaction is symmetric, the coupling has the same constant α when the clock 1 acts on clock 2 and conversely. In our model we assume that α is very small.

All values throughout the paper are in SI units when not explicit.

To prove phase locking we solve sectionally the differential equations (4) with the two small interactions. Then, we construct a discrete dynamical system taking into account the two interactions per cycle seen in Fig. 2 and 3. After that, we compute the phase difference when clock 1 returns to the initial position. The secular repetition of perturbations leads the system to near phase opposition as we can see by the geometrical analysis of Fig. 2 and 3.

The notation is simplified if we consider the function $\gamma(\varphi)$ such that

$$\gamma(x, y) = \begin{cases} \frac{h^2 y}{8\mu} + \frac{2\mu}{y}, & \text{if } 0 \leq x < \frac{\pi}{2}, \\ \frac{h^2 y}{8\mu}, & \text{if } \frac{\pi}{2} \leq x < \frac{3\pi}{2}, \\ \frac{h^2 y}{8\mu} - \frac{2\mu}{y}, & \text{if } \frac{3\pi}{2} \leq x < 2\pi, \end{cases} \quad (5)$$

and the function $\chi(\varphi)$ such that

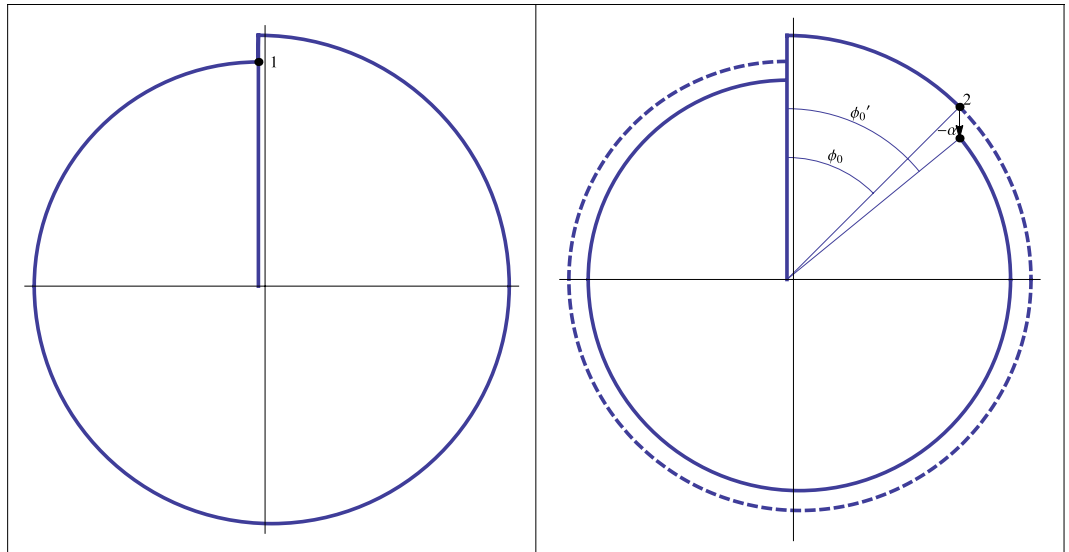


Figure 2. Interaction of clock 1 on clock 2 at $t=0^+$. We see the original limit cycle, before interaction, and the new one in solid and the original limit cycle in dashed. Note that the value of α and of h are greatly exaggerated to provide a clear view. The effect of the perturbation is secular and cumulative.

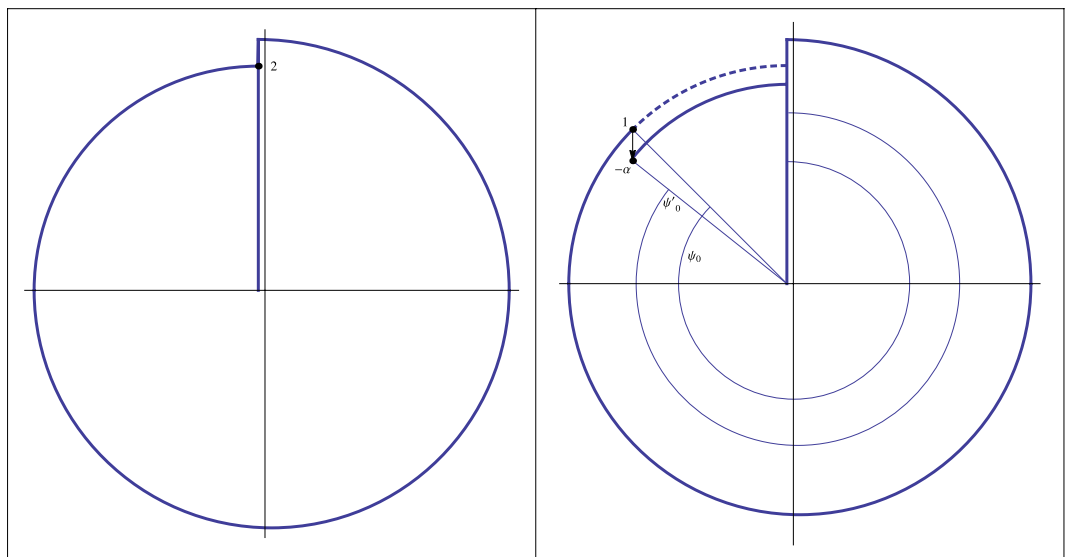


Figure 3. Second interaction. Interaction of clock 2 on clock 1 when clock 2 reaches its impact position. All the features are similar to the Fig. 2.

$$\chi(x, y) = \begin{cases} -\frac{\mu}{y^2}, & \text{if } 0 \leq x < \frac{\pi}{2}, \\ \frac{\mu}{y^2}, & \text{if } \frac{\pi}{2} \leq x < \frac{3\pi}{2}, \\ -\frac{\mu}{y^2}, & \text{if } \frac{3\pi}{2} \leq x < 2\pi. \end{cases} \quad (6)$$

We make the assumption that the natural frequencies are near. A difference of 28 s per day in the movement of the clocks with natural periods in the order of 1.42 s, which is easy to obtain even with very poor clocks, means that ε is on the order of 10^{-3}rads^{-1} .

This means that, in each cycle of each clock, the other one will give one perturbative kick to the other. Suppose that the clocks are brought to contact at $t_0=0$. Consider that the fastest clock (number 1) is at position

$$q_1(0^-) = -\frac{\mu}{\omega + \varepsilon}, \dot{q}_1(0^-) = \frac{h^2\omega + \varepsilon}{8\mu} - \frac{2\mu}{\omega + \varepsilon}. \tag{7}$$

Using γ and χ we have

$$\begin{cases} q_2(0^-) = \frac{\gamma(\phi_0, \omega - \varepsilon)}{\omega - \varepsilon} \sin \phi_0 + \chi(\phi_0, \omega - \varepsilon), \\ \dot{q}_2(0^-) = \gamma(\phi_0, \omega - \varepsilon) \cos \phi_0. \end{cases} \tag{8}$$

The perturbation of clock 1 on clock 2 adds the value of $-\alpha$ to the velocity $\dot{q}_2(0^-)$, keeping the position $q_2(0^-)$. Thus, the new initial conditions at $t=0^+$ for the movement of the second clock are

$$\begin{cases} q_2(0^+) = \frac{\gamma(\phi_0, \omega - \varepsilon)}{\omega - \varepsilon} \sin \phi_0 + \chi(\phi_0, \omega - \varepsilon), \\ \dot{q}_2(0^+) = \gamma(\phi_0, \omega - \varepsilon) \cos \phi_0 - \alpha. \end{cases} \tag{9}$$

The new phase of clock 2, which is the phase difference of the two clocks ϕ'_0 , at 0^+ is now

$$\phi'_0 = \Phi_2(t_0^+) = \arctan \left(\sin \phi_0, \cos \phi_0 - \frac{\alpha}{\gamma(\phi_0, \omega - \varepsilon)} \right). \tag{10}$$

To simplify the notation we consider the function

$$\arctan \left(\sin \phi_0, \cos \phi_0 - \frac{\alpha}{\gamma(\phi_0, \omega)} \right) = \varsigma(\phi_0, \omega, \alpha), \tag{11}$$

therefore

$$\Phi_2(t_0^+) = \varsigma(\phi_0, \omega - \varepsilon, \alpha). \tag{12}$$

With power expansion in α

$$\Phi_2(t_0^+) = \phi_0 + \sum_{n \geq 1} \frac{\sin n\phi_0}{n(\gamma(\phi_0, \omega - \varepsilon))^n} \alpha^n. \tag{13}$$

The correction of the phase difference at $t_0^+ = 0^+$ is

$$\Delta\phi(t_0^+) = (\Phi_2^+(t_0^+) - \Phi_1(0)) - \phi_0 \tag{14}$$

$$= \sum_{n \geq 1} \frac{\sin n\phi_0}{n(\gamma(\phi_0, \omega - \varepsilon))^n} \alpha^n. \tag{15}$$

With first order term in α

$$\Delta_1\phi(t_0^+) \alpha = \frac{\sin \phi_0}{\gamma(\phi_0, \omega - \varepsilon)} \alpha. \tag{16}$$

Now, both clocks start their natural movement.

We suppose that the clock 2 arrives at the vertical position without being overtaken by clock 1, if that is the case we begin our study after that situation occurs. Clock 2 takes the time $\frac{2\pi - \phi_0 - \Delta\phi(t_0^+)}{\omega - \varepsilon}$ to arrive at this position. The phase of clock 2 is $\Phi_2\left(\frac{2\pi - \phi_0 - \Delta\phi(t_0^+)}{\omega - \varepsilon}\right) = 2\pi$. The phase of clock 1 is now

$$\Phi_1\left(\frac{2\pi - \phi_0 - \Delta\phi(t_0^+)}{\omega - \varepsilon}\right) = (2\pi - \phi_0 - \Delta\phi_0) \frac{\omega + \varepsilon}{\omega - \varepsilon}. \tag{17}$$

The next interaction is given by the kick from clock 2 to clock 1. Denoting the phase of clock 1 at this stage by

$$\varphi_0 = (2\pi - \phi_0 - \Delta\phi(t_0^+)) \frac{\omega + \varepsilon}{\omega - \varepsilon} \tag{18}$$

and $t_1 = \frac{2\pi - \phi_0 - \Delta\phi(t_0^+)}{\omega - \varepsilon}$, we have the phase difference immediately before the second kick

$$\Phi_2(t_1) - \Phi_1(t_1) = 2\pi - \varphi_0. \tag{19}$$

The next interaction is given by the kick from clock 2 to clock 1. Using a process similar to the previous kick we have after the second kick

$$\Phi_1(t_1^+) = \varsigma(\varphi_0, \omega + \varepsilon, \alpha). \tag{20}$$

Expanding this function in power series we have

$$\Phi_1(t_1^+) = \varphi_0 + \sum_{n \geq 1} \frac{\sin n\varphi_0}{n(\gamma(\varphi_0, \omega + \varepsilon))^n} \alpha^n. \tag{21}$$

The new phase difference is

$$\Phi_2(t_1) - \Phi_1(t_1^+) = 2\pi - \varsigma(\varphi_0, \omega + \varepsilon, \alpha) \tag{22}$$

$$= 2\pi - \varphi_0 - \sum_{n \geq 1} \frac{\sin n\varphi_0}{n(\gamma(\varphi_0, \omega + \varepsilon))^n} \alpha^n. \tag{23}$$

The correction of the phase difference at t_1^+ is now

$$\Delta\phi(t_1^+) = - \sum_{n \geq 1} \frac{\sin n\varphi_0}{n(\gamma(\varphi_0, \omega + \varepsilon))^n} \alpha^n, \tag{24}$$

with first order term in α

$$\Delta_1\varphi(t_1^+) \alpha = - \frac{\sin \varphi_0(\phi_0)}{\gamma(\varphi_0(\phi_0), \omega + \varepsilon)} \alpha, \tag{25}$$

and this expression can be further simplified remembering that

$$\varphi_0(\phi_0) = (2\pi - \phi_0 - \Delta\phi_0) \frac{\omega + \varepsilon}{\omega - \varepsilon}, \tag{26}$$

giving in first order in α

$$\Delta_1\varphi(t_1^+) \alpha = \frac{\sin \phi_0}{\gamma(\phi_0, \omega + \varepsilon)} \alpha. \tag{27}$$

To complete the study of the phase difference the clock 1 must return to the vertical position, which happens for the time t_2^- . The time that this clock takes to return to the vertical position is $\frac{2\pi - \Phi_1(t_1^+)}{\omega + \varepsilon}$, the phase of clock 1 is now 2π , the phase of clock 2 gives us the new phase difference ϕ_1 after one cycle of clock 1, that is

$$\phi_1 = \Phi_2(t_2^-) - \Phi_1(t_2^-) \tag{28}$$

$$= 2\pi + (2\pi - \Phi_1(t_1^+)) \left(\frac{\omega - \varepsilon}{\omega + \varepsilon} \right) - 2\pi. \tag{29}$$

$$= (2\pi - \varsigma(\varphi_0, \omega + \varepsilon, \alpha)) \left(\frac{\omega - \varepsilon}{\omega + \varepsilon} \right) \tag{30}$$

$$= \left(2\pi - \varsigma \left((2\pi - \varsigma(\phi_0, \omega - \varepsilon, \alpha)) \frac{\omega + \varepsilon}{\omega - \varepsilon}, \omega + \varepsilon, \alpha \right) \right) \left(\frac{\omega - \varepsilon}{\omega + \varepsilon} \right). \tag{31}$$

If we call the affine function

$$r(x, d) = d(2\pi - x), \tag{32}$$

and the coefficients

$$d_1 = \frac{\omega + \varepsilon}{\omega - \varepsilon} > 1 \text{ and } d_2 = \frac{\omega - \varepsilon}{\omega + \varepsilon} < 1, \tag{33}$$

the large expression (31) is the composition of four maps

$$\phi_1 = r(\varsigma(r(\varsigma(\phi_0, \omega - \varepsilon, \alpha), d_1), \omega + \varepsilon, \alpha), d_2). \tag{34}$$

The discrete dynamical system for $n \geq 0$ is given by the map Ω such that

$$\phi_{n+1} = \Omega(\phi_n) \tag{35}$$

$$= r(\varsigma(r(\varsigma(\phi_n, \omega - \varepsilon, \alpha), d_1), \omega + \varepsilon, \alpha), d_2). \tag{36}$$

Obviously, Ω is a map from the interval $[0, 2\pi]$ to itself. Despite the apparent complexity of Ω , this map is relatively manageable. Under certain conditions we can prove that Ω has a stable fixed point. In this work we deal only with the first degree approximation, relative to the small parameters α and ε , the value of the fixed point ϕ_f which is near to π . The phase difference is asymptotic to the solution φ_f . Knowing this value it is possible to prove the existence and stability of the limit cycle of each clock in interaction and the final asymptotic frequency ω_f . Under this model we can say that Huygens sympathy occurs.

In first order of α and ε we have the iterative scheme

$$\phi_{n+1} = \phi_n + 4\pi \frac{-\varepsilon}{\omega + \varepsilon} + \frac{\alpha \sin \phi_0}{\gamma(\phi_0, \omega - \varepsilon)} + \frac{\alpha \sin \phi_0}{\gamma(\phi_0, \omega + \varepsilon)} \tag{37}$$

$$= \phi_n + 4\pi \frac{-\varepsilon}{\omega + \varepsilon} + \frac{2\alpha \sin \phi_0}{\gamma(\phi_0, \omega)} + h.o.t, \tag{38}$$

We define the map

$$\Xi(x) = x + 4\pi \frac{-\varepsilon}{\omega + \varepsilon} + \frac{2\alpha \sin x}{\gamma(x, \omega)}. \tag{39}$$

We get in first order of α and ε the dynamical system for the phase difference

$$\phi_{n+1} = \Xi(\phi_n) = \phi_n + 4\pi \frac{-\varepsilon}{\omega + \varepsilon} + \frac{2\alpha \sin \phi_n}{\gamma(\phi_n, \omega)}. \tag{40}$$

There are two fixed points ϕ_f^s and ϕ_f^u of Ξ in the interval $[0, 2\pi]$

$$\phi_f^s = \pi - \arcsin \frac{\pi h^2 \varepsilon}{4\alpha \mu}, \quad \phi_f^u = \arcsin \frac{\pi h^2 \varepsilon}{4\alpha \mu}. \tag{41}$$

The derivative of Ξ at the fixed point ϕ_f^s must be $|\Xi'(x_f)| < 1$ to have stability and the condition about the argument of the function arcsin gives

$$\frac{\pi h^2}{4\mu} \varepsilon < \alpha < \frac{h^2 \omega}{8\mu}, \text{ i. e., } \frac{h^2}{8\mu} \pi \Delta \omega < \alpha < \frac{h^2}{8\mu} \omega. \tag{42}$$

Therefore, the limit of the phase difference is, in first order, $\pi - \arcsin \frac{\pi h^2 \varepsilon}{4\alpha \mu}$ which is very near to π when the natural frequencies of both clocks are very near, i.e., small ε . When the system reaches this limit the corrections of phase are null for both clocks.

Simulation

To study the Huygens synchronization we used numerical simulations. We applied the map $\Xi(x)$ without performing the Taylor expansion. We used the environment of Wolfram Mathematica 9.0 to produce the computations. The values of μ, h, ω, t_0 were taken realistically from the experimental setup and kept fixed throughout the simulations. The coupling constant α and the half-difference between the clocks frequencies ε are adjusted in simulations.

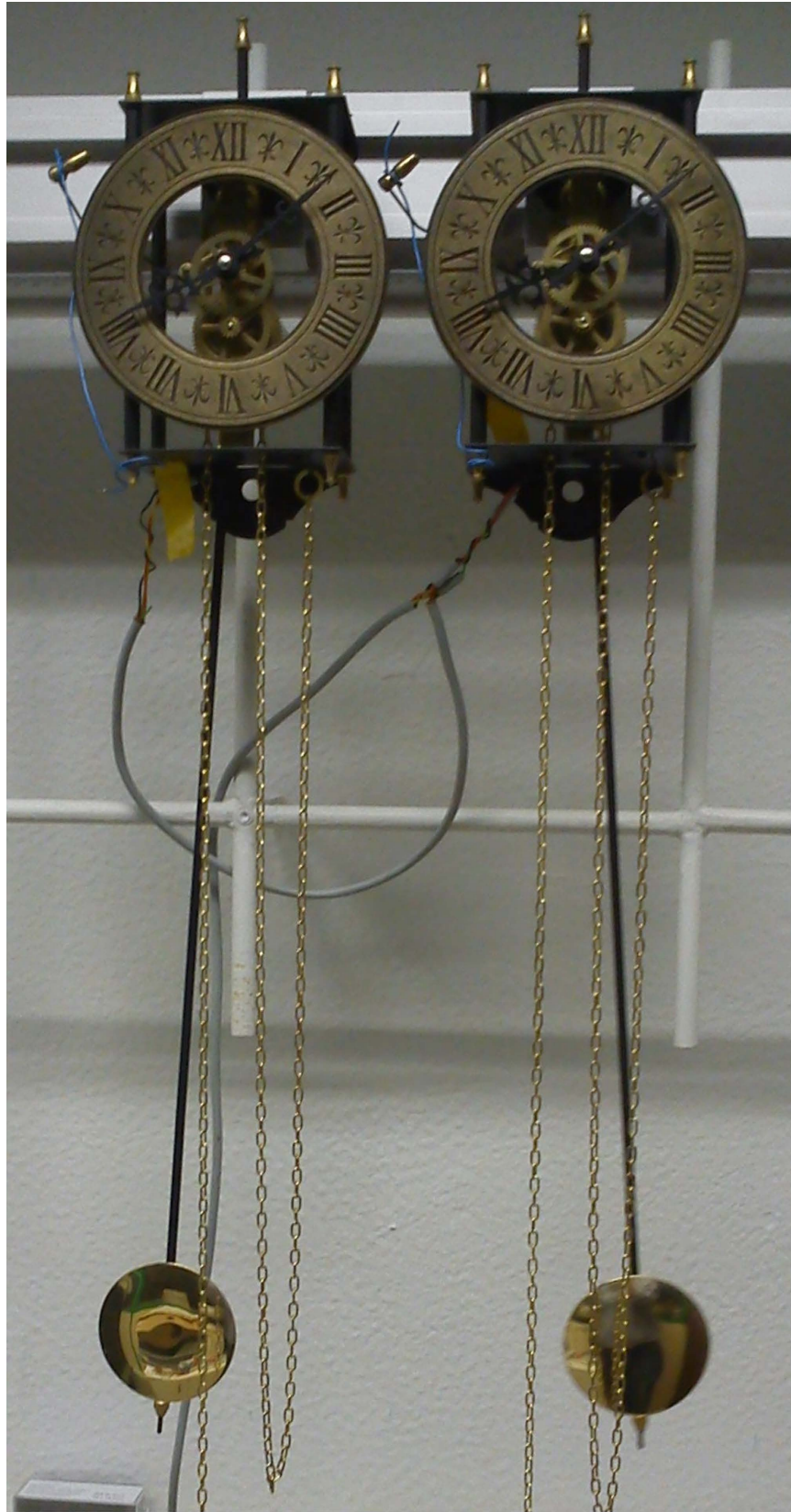


Figure 4. Photo of the experimental setup. The clocks can be seen hanging from the AI rail. The weights are outside of the picture. The cables in the background connect the optical sensors.

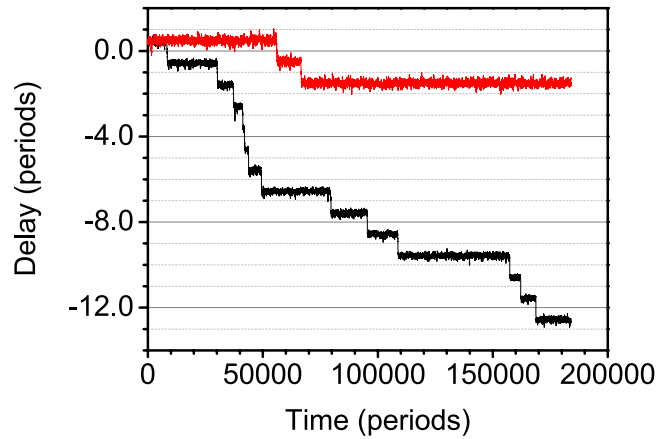


Figure 5. Simulations of delay between the two clocks in period units for two frequency differences. Upper curve (red): $\varepsilon = 1.5 \times 10^{-4}$ rad/s. Lower curve (black): $\varepsilon = 3.0 \times 10^{-3}$ rad/s. $\omega = 4.48799$ rad/s.

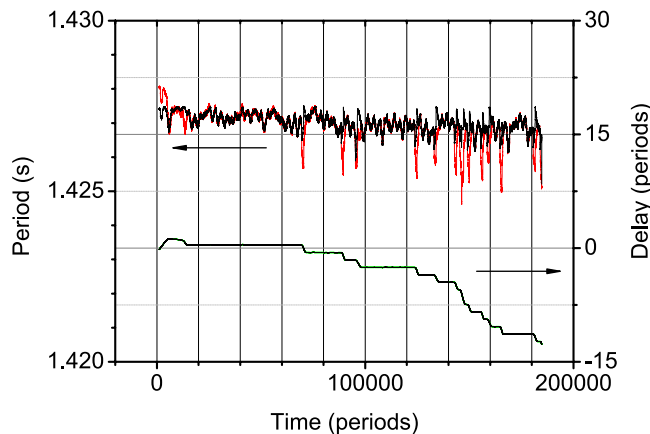


Figure 6. Phase difference between the clocks in period units over more than three days (lower curve in green, right axis) and periods of the two clocks (upper curves, left axis; red for clock 1, black for clock 2). The initial behaviour corresponds to mechanical stabilization of the clocks during the first few hours of the experiment.

Additionally, we introduced noise in the model with normal distribution acting directly on the phase. The effect of noise is to mimic the small perturbations that occur in the lab, e.g., vibrations in the wall and the stochastic changes of the level of the interaction, cycle after cycle. The strength of this stochastic effect is given by the parameter ρ . When the noise function is not used, i.e. $\rho = 0$, if the parameters are in the convergence region given by conditions (42) we have a fixed convergence point of Ω .

Experimental

Experiments were setup using a standard optical rail (Eurofysica) rigidly attached to a wall to which two similar pendulum clocks were fixed through modified rail carriers. This setup can be seen in Fig. 4. The clocks were 230 mm apart. This was the lowest distance still ensuring that the pendulums trajectories were completely separated. The mass-driven anchor-pendulum clocks used were Acctim 26268 Hatahaway. One mass travel supplies energy for around 5 days, and the clocks take about one day to relax to the final frequency after winding. The period, of the order of 1.42 s, is configured by rotating the screw at the bottom of the pendulum, thus changing the actual pendulum length. The chime mechanism was inhibited in order to reduce mechanical noise. Time was measured using one U-shaped LED emitter-receptor TCST 1103, connected to a Velleman K8055 USB data acquisition board operated with custom-developed Visual Basic 6 software running in a standard personal computer (PC). The time measured corresponds to the left maximum angle, and is the midpoint of the interval of the sensor coverage by the pendulum beam. The uncertainty in time acquisition typically expected in the ms range for the PC was overcome by performing running averaging of the period data, up to 1000. The data files were then processed offline using Mathematica. In order to obtain the appropriate parameters for the

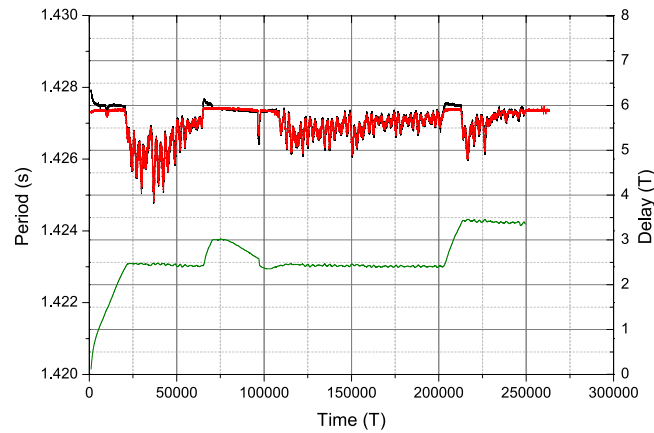


Figure 7. Phase difference between the clocks in period units over more than three days (lower curve in green, right axis) and periods of the two clocks (upper curves, left axis; red for clock 1, black for clock 2). The initial behaviour corresponds to mechanical stabilization of the clocks during the first few hours of the experiment. After running for around 250000 periods, clock 2 is stopped, and clock 1 keeps running undisturbed.

simulation, the pendulums were filmed and the movement quantified using free software *Tracker4.84* (last date of access: 27/03/2015) from OSP <https://www.cabrillo.edu/~tracker>.

We assume that the coupling is obtained through the exchange of sound pulses between the clock propagated through the rail. This is consistent with the absence of coupling for other materials tried (MDF and fiberglass). The exact mechanism of how the pulse energy propagates through the clock hardware down to the pendulum is hard to assess in detail and depends on the individual clock. The sound propagation speed in Al is 6420 ms^{-1} , leading to a propagation time of the order of $3.0 \times 10^{-5} \text{ s}$, which is negligible in face of the 1.42 s period of the oscillators, and so the instantaneous propagation of sound assumed in the model is a reasonable approximation.

Results and discussion

Observing the movement of the pendulum alone (as a damped oscillator; initially at the limit cycle), we noticed a decrease of the maximum velocity of the pendulum according to a linear fit $v_{\text{max}} = 0.2228 - 0.0023n$, where n is the number of cycles, with correlation coefficient 0.994. The decrease of velocity per cycle predicted by the Andronov model is $\frac{4\mu}{\omega}$. With the value of the period $T = 1.40000 \text{ s}$ and $\omega = \frac{2\pi}{T} = 4.48799 \text{ rad/s}$, we can estimate the value of $\mu = \frac{\omega \Delta v}{4} \approx 2.54 \times 10^{-3}$.

The value of h can also be easily established by studying the movement at the limit cycle. We then have the maximum velocity $v_f = \frac{h^2 \omega}{8\mu} + \frac{2\mu}{\omega}$. We found consistently that the maximum velocity at the limit cycle is $v_f = 0.223 \text{ m/s}$. Therefore, $h \approx 0.032$.

We used different possible values of natural frequency difference. For the average natural angular frequency we take the same value of $T = 1.40000 \text{ s}$, hence $\omega = 4.48780 \text{ rad/s}$. The fastest clock has a natural frequency of $\omega + \varepsilon$ and the slowest $\omega - \varepsilon$. The angular frequency difference is in first order $\varepsilon = \frac{2\pi}{T^2} \Delta t$, where Δt is half of the period difference. Notice that when $\Delta t = 2 \times 10^{-4} \text{ s}$, with a delay between the clocks of 24.6 s per day for the non coupled pair of clocks, the value of ε is $\varepsilon = 6.4 \times 10^{-4} \text{ rad/s}$. We used values of ε in the range 10^{-4} to 10^{-3} rad/s as a realistic estimate for the performance of our setup.

The fixed parameters used for the simulations are then $\mu = 2.54 \times 10^{-3}$, $h = 0.032$, $\omega = 4.48799 \text{ rad/s}$, $t_0 = 0.8\pi \text{ s}$, and the phenomenological noise coefficient of $\rho = 0.093$, which fits the ripple observed at the experimental data. When we choose $\varepsilon = 3 \times 10^{-3} \text{ rad/s}$, corresponding to a huge natural delay of 116 s per day with the clocks in the isolated state, a value of $\alpha = 7 \times 10^{-4}$ yielded results matching the experimental data. The conditions (42), using the linear approximation, give an estimate threshold of $\varepsilon = 2.2 \times 10^{-3} \text{ rad/s}$ for the coupling with the same values of the fixed parameters. This is not contradictory with our results, since we used in the simulations the function Ξ with no approximations and we found numerically that the actual threshold for that function is at $\varepsilon = 3.5 \times 10^{-3} \text{ rad/s}$.

We expect more frequent escapes from stable states than if we choose $\varepsilon = 1.5 \times 10^{-4} \text{ rad/s}$, corresponding to a natural delay of 2.9 s per day. These values correspond to the values that could realistically be obtained in our experimental setup. The plots can be seen in Fig. 5.

Notice the small differences assumed for the frequencies, of the same order of the values measured for independent clocks. The time difference stabilizes in horizontal plateaus, corresponding to phase opposition coupling. The stochastic term introduced in the simulation unsets the system at some point, and then the phase difference increases quickly as the fastest clock runs away until the next synchronization plateau is reached, one or sometimes two periods away. For the simulation with the smaller difference

between frequencies, the number of transitions between plateaus is smaller, as expected since the stability is much easier to reach and maintain.

This is strikingly similar to the behaviour observed in Fig. 6 for the actual clocks (right axis). The number of synchronization plateaus is of the same order and can be fine-tuned using the stochastic parameter in the simulation. It was observed that the system could be unsettled by a number of external noise sources, e.g. from doors closing nearby in the building, people entering or leaving the room, or even the elevator stopping, than proceeding to the next synchronization plateau.

The periods of both clocks from the same experiment can be seen on the same figure (left axis). The periods vary together within an interval of about 1 ms around 1.427 s when the clocks are coupled with correlation coefficient above 0.97 in the coupled state. Notice the almost perfect coincidence of the two curves except when the system leaves coupled states. Notice also the unstability of the coupled period, varying over an interval of almost 1 ms. When coupling is lost the period of one clock decreases sharply (up to 2 ms or more) and the period of the other clock increases by a (smaller) amount. These perturbations in the periods are coincident with the loss of phase opposition coupling. Although one may expect changes in the frequency even when the clocks are not coupled, due to the interaction between them, the difference in period can be estimated at around 2 ms, corresponding to a difference in frequency of the order of 6×10^{-3} rad/s. This asymmetry of the coupled period relative to the original periods is predicted by the model. Both periods return to the previous baseline value when the coupling is restored.

Fig. 7 shows data for another experiment. In this case the free clock frequencies were closer. Both periods are remarkably coincident, but vary in an interval in excess of 10 ms, when the clocks are coupled. Since the frequencies are closer, the synchronization should be easier to maintain, hence the low number of plateaus, but also should be slower to attain, hence the longer transitions between plateaus. If the perturbation is large enough, especially if the frequencies are very close, it is possible to attain plateaus both above and below. Between $t = 100000 T$ and $t = 112000 T$ approximately the synchronization is lost, and the periods become separated by more than 100 μ s (corresponding to frequency difference around 3×10^{-4} rad/s), but become stable (within 1 s). At instant $t = 148000 T$ approximately clock #2 is stopped. From that moment on the period of the remaining working clock becomes stable within about 10 s, an interval one order of magnitude below. This confirms that the clocks strongly disturb one another, but also that both periods are kept at the same value in order to keep the synchronization at the expense of some frequency unstability.

Conclusions

We have developed a model explaining the Huygens problem of synchronization between two clocks hanging from a wall. In this model each clock transmits once per cycle a sound pulse that is translated in a pendulum speed change. An equilibrium situation is obtained for almost half-cycle phase difference. These predictions match remarkably the experimental data obtained for two similar clocks hanging from a wall.

References

- Huygens, C. *Letters to de Sluse*, (letters; no. 1333 of 24 February 1665, no. 1335 of 26 February 1665, no. 1345 of 6 March 1665) (Societe Hollandaise Des Sciences, Martinus Nijho, 1895).
- Bennett, M., Schatz, M., Rockwood, H. & Wiesenfeld, K. Huygens' clocks. *P Roy Soc Lond A Mat* **458**, 563–579 (2002).
- Czolczynski, K., Perlikowski, P., Stefanski, A. & Kapitaniak, T. Huygens' odd sympathy experiment revisited. *Int J Bifurcat Chaos* **07**, 2047–2056 (2011).
- Kapitaniak, M., Czolczynski, K., Perlikowski, P., Stefanski, A. & Kapitaniak, T. Synchronization of clocks. *Phys Rep* **1**, 1–69 (2012).
- Fradkov, A. & Andrievsky, B. Synchronization and phase relations in the motion of two-pendulum system. *Int J Nonlinear Mech* **6**, 895–901 (2007).
- Jovanovic, V. & Koshkin, S. Synchronization of Huygens' clocks and the Poincare method. *J Sound Vib* **12**, 2887–2900 (2012).
- Martens, E. A., Thutupalli, S., Fourrière, A. & Hallatschek, O. Chimera states in mechanical oscillator networks. *P Natl Acad Sci USA* **26**, 10563–10567 (2013).
- Oud, W. T., Nijmeijer, H. & Pogromsky, A. Y. *A study of Huijgens' synchronization: experimental results*, vol. 336 of *Lecture Notes in Control and Information Science*, 191–203 (Springer, 2006).
- Senator, M. Synchronization of two coupled escapement-driven pendulum clocks. *J Sound Vib* **3-5**, 566–603 (2006).
- Abraham, R. & Garfinkel, A. The dynamics of synchronization and phase regulation (2003). URL <http://www.ralph-abraham.org/articles/Blurbs/blurb111.shtml>. (Date of access: 27/03/2015).
- Abraham, R. *Phase regulation of coupled oscillators and chaos*, 49–78 (World Scientific, 1991).
- Nunes, A. M. & Vassalo-Pereira, J. Phase-locking of two Andronov clocks with a general interaction. *Phys Lett A* **8**, 362–366 (1985).
- Vassalo-Pereira, J. A theorem on phase-locking in two interacting clocks (the Huygens effect). In Avez, A., Blaquièrre, A. & Marzollo, A. (eds.) *Dynamical Systems and Microphysics: Geometry and Mechanics*, 343–352 (Academic Press, 1982).
- Pikovsky, A., Rosenblum, M. & Kurths, J. *Synchronization: A Universal Concept in Nonlinear Sciences*, vol. 12 of *Cambridge Nonlinear Science Series* (Cambridge University Press, 2003).
- Andronov, A. A., Vitt, A. A. & Khaikin, S. E. *Theory of Oscillators* (Pergamon Press, 1966).
- Birkhoff, G. D. *Collected Mathematical Papers* (American Mathematical Society, 1950).

Acknowledgements

Funded by FCT/Portugal. H.M.O. by project PEst-OE/EEI/LA0009/2013 for CMAGDS and L.V.M by project PEst-OE/CTM/LA0024/2013 for INESC-MN and IN.

Author Contributions

H.M.O. and L.V.M. wrote the main manuscript text and prepared the figures in equal parts. Both authors reviewed the manuscript. Both authors contributed equally to the paper.

Additional Information

Competing financial interests: The authors declare no competing financial interests.

How to cite this article: Oliveira, H. M. and Melo, L. V. Huygens synchronization of two clocks. *Sci. Rep.* **5**, 11548; doi: 10.1038/srep11548 (2015).



This work is licensed under a Creative Commons Attribution 4.0 International License. The images or other third party material in this article are included in the article's Creative Commons license, unless indicated otherwise in the credit line; if the material is not included under the Creative Commons license, users will need to obtain permission from the license holder to reproduce the material. To view a copy of this license, visit <http://creativecommons.org/licenses/by/4.0/>